D1.2: WP1 research report I

Project Name: Future Optical Networks for Innovation Research and Experimentation
Acronym: ONFIRE
Project no.: 765275

Start date of project: 01/10/2017 **Duration:** 42 Months

This project has received funding from the European Union's Horizon 2020 research and innovation programme under the Marie Skłodowska-Curie Actions.

Document Properties

Document ID	EU-H2020-MSCA-ITN-2017-765275-ONFIRE-D1.2
Document Title	*D1.2 – WP1 research report I*
Contractual date of delivery to REA	*30/11/2018*
Lead Beneficiary	Centre Tecnològic de Telecomunicacions de Catalunya (CTTC)
Editor(s)	Fabiano Locatelli (ESR1)
Work Package No.	1
Work Package Title	Disaggregated Optical Networks
Nature	Report
Number of Pages	56
Dissemination Level	**PUBLIC**
Contributors	CTTC: Josep Maria Fàbrega, Michela Svaluto Moreolo, Raul Munoz Nokia: Konstantinos Christodoulopoulos, Lars Dembeck UPC: Salvatore Spadaro
Version Nr.	1

Executive summary

This document presents a general review of the research progress made by the ESR1 during his first year in the ONFIRE project.

After being selected for ONFIRE programme, the ESR1 has joined CTTC in Barcelona, Spain on May 2018, and then has moved to Nokia Bell Labs in Stuttgart, Germany on February 2019, where he is currently hosted.

The activities carried out by ESR1 during this first year mainly focused on the analysis of the state of the art and the draft of his research plan proposal. Following that, the ESR1 has worked on the design and the assessment of cost-effective schemes for high-resolution spectrum analysis and on the development of a machine learning-based ONSR estimation tool.

A detailed description of all these activities is presented within this report.

Contents

List of Figures

1 INTRODUCTION

1.1 DOCUMENT OBJECTIVES AND STRUCTURE

This report is intended to give an in-depth view on what the Early Stage Researcher 1 (ESR1) has achieved so far in the framework of the Horizon 2020 Marie Skłodowska-Curie Actions, ONFIRE (Future Optical Networks for Innovation, Research and Experimentation) project. ESR1, Fabiano Locatelli, joined the Optical Networks and Systems Department of "Centre Tecnològic de Telecomunicacions de Catalunya" (CTTC) in Barcelona (Spain) and the ONFIRE project on May 2018, after being selected for the position on April 2018. On February 2019, he moved to Nokia premises in Stuttgart for the first scheduled secondment period. He is currently performing the planned activities there within the IP and Optical Networking Department of the Smart Optical Fabric & Device Lab.

The goals achieved so far by the ESR1 in relation to those initially planned are listed in the following lines. Since he has started, the ESR1 performed the following main tasks:

- Analysis of the state of the art (SoA) and research plan proposal [1]. The research plan envisions to carry out research on 3 different topics: optical performance monitoring and more specifically optical signal-to-noise ratio monitoring, low margin optical networks and disaggregated optical networks.
- Design and assessment of cost-effective schemes for high-resolution spectrum analysis in order to perform optical performance monitoring agnostic to the modulation format, according to the research plan.
- Development of a tool to process pre-collected optical spectra and extract their main parameters (OSNR, central frequency, 3dB-bandwidth).
- Development of a machine learning-based OSNR estimator from optical spectra: the results of this work have been gathered in a letter, submitted in June 2019 to the IEEE Photonics Technology Letters [2] and currently under revision.
- Contributor to and leading writer of several project deliverables: deliverable D1.1 "Consolidated state of the art survey and individual research proposal of ESR1" [1] (leader), deliverable D4.5 "Progress report" [3], and deliverable D1.2 "Research report I" (leader).

During the past months, the ESR1 was also involved in the preparation of his thesis proposal plan titled "Data Plane Architectures and Monitoring Techniques for System Margins Reduction in Disaggregated Optical Networks", which was presented in January 2019 to the UPC commission. In the same month, in addition, a talk at CTTC in the context of "CTTC Weekly Seminar Series" was given by ESR1 with the title "Data Plane Technologies for Disaggregated Optical Networks".

This document is organized as follows. Section 2 presents a brief summary of what was included in the deliverable D1.1 [1], namely a deep revision of the SoA of the three main topics: low-margin optical networks, OSNR monitoring techniques and disaggregated networks. In section 3, we present the investigation over new possible schemes for high-resolution optical spectral sensing. In the same direction, Section 4 illustrates how the captured optical spectral data can be processed and analysed with and without the aid of

machine learning [2]. In section 5, we outline our conclusions over the achieved work together with the possible future envisioned steps. Finally, Appendix A gives a detailed overview of the algorithm developed for spectral analysis.

2 INTRODUCTION TO OSNR MONITORING, LOW-MARGIN AND DISAGGREGATED OPTICAL NETWORKS

In the deliverable D1.1 [1] we presented the current SoA of three main subjects: ONSR monitoring techniques, low-margin optical networks and disaggregated optical networks. With the aim to provide some background information for the following sections, in this paragraph a brief overview of the above-mentioned topics is reported.

2.1 OPTICAL SIGAL-TO-NOISE MONITORING

To close the so-called cognition cycle of the network, the optical performance monitoring (OPM) techniques must deliver the feedback needed to guarantee the quality of the transmission. Thus, common subsystems agnostic of the signal waveforms or of the modulation formats should be investigated to improve the existing optical performance monitoring techniques.

Among all the available monitorable parameters, one of the most important to consider is the optical signal-to-noise ratio (OSNR), because it is transparent to both the bit rate and modulation format and is also directly correlated to the BER [4]. OSNR gives a measure of the amplified spontaneous emission (ASE) noise introduced by optical amplifiers (like EDFAs): ASE affects the receiver ability to properly decode the optical signal and thus introduces errors. It can be quantified in terms of OSNR as [4]:

$$OSNR = 10\log\left(\frac{P_s}{P_n}\right) + 10\log\left(\frac{B_m}{B_r}\right)$$

where:

- P_s represents the power of the optical signal
- P_n represents the power of the optical noise
- B_m represents the noise equivalent bandwidth (NEB) of the OSA
- B_r represents the measured resolution bandwidth (RBW)

The most common approach for OSNR measurement relies on linear interpolation (LI), where the noise level of each peak (corresponding to the operating wavelength of each channel) of the optical spectrum is estimated interpolating the noise power levels measured at the two adjacent peaks. This technique could fail in case of wavelength switched optical networks, where each channel may experience a different amount of ASE noise with respect to the other channels, as shown in Fig. 1, or in case of very tight wavelength division multiplexed (WDM) channel spacing, where strong filtering effects are present.

So far, several techniques have been proposed to overcome these problems; we can split them into two main categories. The first includes the so-called linear and non-linear approaches, which are cost-effective and bit rate transparent, such as the polarization-based (PB) techniques [5], the interferometer-based (IB) technique [6], the beat noise analysis-based (BNA) techniques [7], the optical amplifiers operating condition-based (OA) technique [8] and the amplitude histograms-based (AH) techniques [9] [10]. The main issues of these solutions are their incompatibility with polarization multiplexed (PM) signals (for PB techniques), or their dependency on transmission distortions such as: polarization

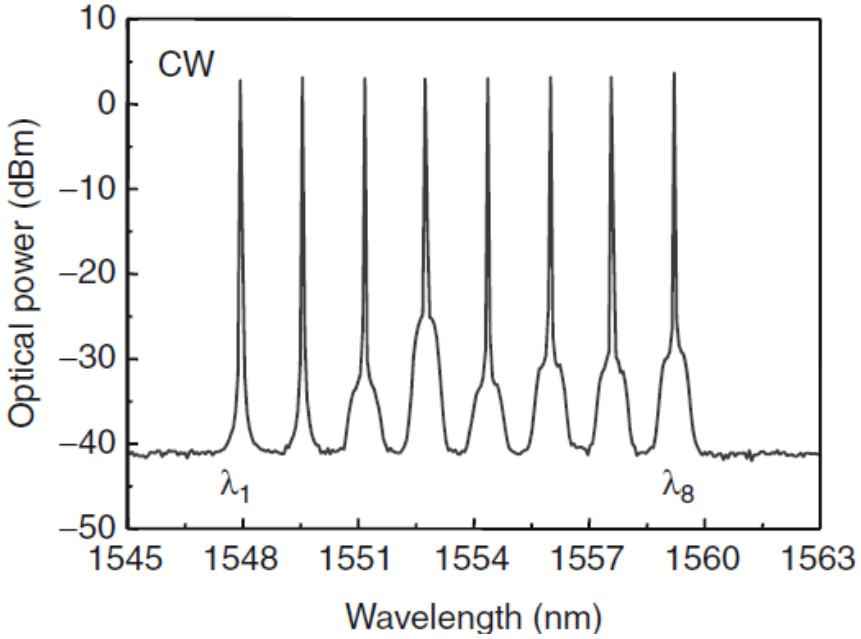

Fig. 1. Optical spectrum of unmodulated continuous waveform signals with eight wavelength channels. It is easily observable how the ASE noise levels vary with the wavelength. Reproduced from [11].

mode dispersion (PMD), non-linear birefringence (NLB), polarization dependent loss (PDL) and chromatic dispersion (CD) [12]. On the other hand, the second category includes the OSNR monitoring techniques based on the digital signal processing (DSP) of coherent receivers [13]. In this case, all the previous transmission distortion related issues can be compensated by the DSP, but only in presence of coherent receivers, which are a costly and impractical solution especially for monitoring at intermediate nodes of the network [12].

2.2 LOW-MARGIN OPTICAL NETWORKS

In optical networks, margins ensure the network's operations even in the event of failures or degradation of its elements. Margins are demanded by operators and accounted for by the network equipment providers [14]. They typically take values of several dB (e.g. 3-4dB). The margin of a lightpath is assessed as the difference between the actually quality of transmission (QoT) metric of the signal and the threshold above which the signal is considered recoverable without errors (i.e. FEC limit). When too large, the margins provisioned during the network deployment or when a new lightpath is deployed can significantly shorten the transmission reach of the channel. Therefore, to increase the efficiency of the networks, the margins should be minimized by understanding the physical network state and reducing them without affecting the resilience/availability of the connections.

Three types of margins were defined [15]: unallocated margins (U-margins), design margins (D-margins) and system margins (S-margins). The former are known before the network deployment and come from the mismatch between the demanded capacity and reach (source-destination distance) demand, and the equipment capability. On the other hand,

D-margins are defined as the difference between the planned and the real performance of the deployed network; they typically take into account the uncertainties due to inaccuracies of the design tools used to evaluate the QoT and the inaccuracies of the inputs of this QoT tool. Unlike the U-margins case, their impact is only known at deployment time. Finally, the S-margins take into account impairments and line degradation, such as polarization effects (a fast-varying impairment), increasing nonlinearities (network utilization is light at the beginning of its life and increase as more connections are established) and network elements aging (e.g. transponder aging, amplifier noise factor aging, fiber aging, etc.): both of the latter two factors are considered as slow-varying impairments. Furthermore, S-margins also may include an additional arbitrary operator margin. Likewise D-margins, S-margins are only known after network deployment and unlike both the other two margins types, they may vary with time.

2.3 DISAGGREGATED NETWORKS

Thanks to the rise of technologies such as software-defined networking (SDN) and network functions virtualization (NFV), the telecom industry is moving from a convergence approach, where functions that once resided in separate devices were merged in single systems, towards a more dynamic and flexible scenario: the networks disaggregation [16] [17]. Since the disaggregation approach implies a functional disaggregation rather than a block-by-block one [18], different data plane aspects must be redesigned. To do so, an evolution from chassis-based (proprietary) network elements to commodity (off-the-shelf) components, the so-called *white boxes*, is required. Within the white-boxes paradigm, generic off-the-shelf hardware can be purchased from any vendor and customized with software from different sources, thus allowing the operators to size their infrastructure as needed [19]. White-box model is the evolution of the *bare metal* operational mode, where the operators source their hardware supplies directly from the original design manufacturers (ODMs) and adapt free and open source software to it [20]. On the other hand, with the so-called *black box* approach, the single vendor closely aggregates both the hardware and software and assumes oversight of hardware components. Finally, in the middle between white and black box paradigms there is *brite box* operational model (i.e. branded white box HW), where, as in white boxes, the operating system and application software are disaggregated from the hardware and also come provisioned for a tailored level of lifecycle support from the vendor.

2.4 RELATION BETWEEN THE SOA AND THE PROPOSED WORK

The following sections describe the work in which the ESR1 has been involved so far, which is mainly related to the OSNR monitoring task. Indeed, a new way to estimate the OSNR, which also involves machine learning, will be proposed. Since the OSNR knowledge can help understanding the network current state, the proposed OSNR monitoring technique could also have a crucial impact on the network margins reduction. In addition, the optical performance monitoring play an even more fundamental role in disaggregated network scenarios, where the network margins are harder to define with respect to the classic aggregated approach.

Undoubtedly, the envisioned future steps (see Section 5) will be more focused on the disaggregated optical networks approach and on the margin reduction techniques.

3 HIGH-RESOLUTION OPTICAL SPECTRUM SENSING FOR PERFORMANCE MONITORING

In the previous section we saw that the OSNR is considered the most common parameter to be monitored for signal quality measurement purposes: it is transparent to the bit rate and modulation format and it can be easily correlated to the BER. Nowadays, very high-resolution optical spectrometry solutions are available on the market, as for example the Brillouin Optical Spectrum Analyser (BOSA) [20]. This device works exploiting the stimulated Brillouin scattering (SBS), a non-linear optical effect that causes a very narrow filtering [22], which allows the BOSA to achieve high optical rejection ratio and resolution up to 10 MHz (see Fig. 2). However, these options are bulky and expensive; thus, new cost-effective and more compact solutions should be investigated. Indeed, the purpose of this section is to describe the work carried out by ESR1, on investigating new possible approaches for high-resolution optical spectrum analysis.

A first approach consists on increasing the resolution of an optical spectrum measurement by using a known and programmable external signal that can slice a generic signal-under-test (SUT). A first attempt has been carried out modulating the SUT with an electric radio-frequency OFDM real-valued signal, by means of an external Mach-Zehnder modulator (MZM).
Referring to Fig. 3, the real-valued OFDM signal can be represented as [23]

$$s(t) = \sqrt{\frac{\sigma_s^2}{N_c}} \sum_{k=1}^{N_c} Re\{X_k\} \cos(2\pi k \Delta f t)$$

where
- σ_s^2 represents the mean power of $s(t)$
- N_c represents the number of subcarriers of the OFDM signal, which is equal to

$$N_c = \frac{N_{FFT}}{2} - 1$$

- N_{FFT} represents the length of the inverse fast Fourier transform (FFT) at the OFDM modulator
- $Re\{X_k\}$ represents the real part of the complex data symbols X_k
- Δf represents the frequency spacing between two subcarriers.

On the other hand, the SUT $x(t)$, is the optical signal fed into the optical input of the MZM, and can be represented as

$$x(t) = \sqrt{P(t)} e^{j2\pi f_o t}$$

where
- $P(t)$ represents the power of $x(t)$
- f_o represents the optical carrier frequency.

At the output of the MZM, the optical field can be expressed as [23]

$$E_{MZM}(t) = \sqrt{P(t)} \cdot \cos\left(\frac{\pi}{2} \frac{s(t) + V_{BIAS}}{V_\pi}\right) e^{j2\pi f_o t}$$

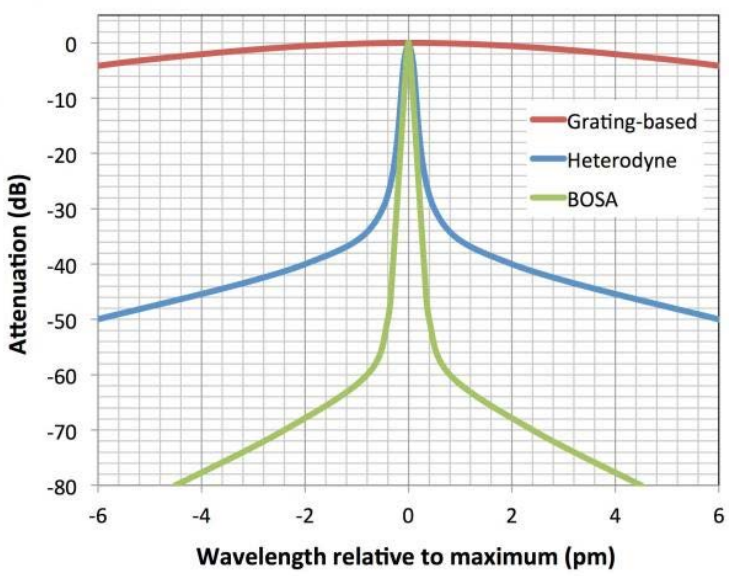

Fig. 2. Comparison between the high-resolution BOSA spectrum analysis (green line) and other possible approaches. Reproduced from [22].

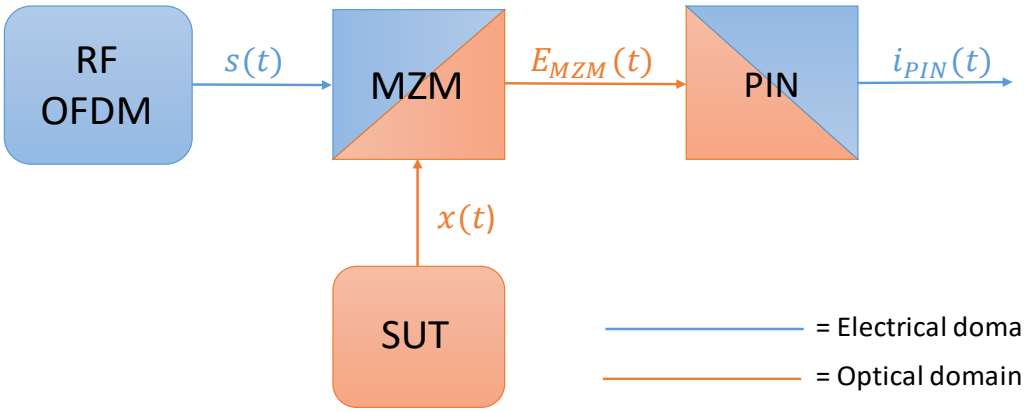

Fig. 3. Simplified block diagram of the proposed scheme. RF-OFDM: radio-frequency OFDM signal, MZM: Mach-Zehnder modulator, SUT: optical signal-under-test, PIN: PIN photodiode.

where

- V_{BIAS} represents the MZM bias voltage
- V_π represents the MZM switching voltage.

To operate the MZM as a pure intensity modulator, it has to work in the so-called push-pull configuration. To do so, the MZM must be biased at its quadrature point (i.e. V_{BIAS} should assume the value of $V_\pi/2$).

After few mathematical steps, the formulation of the MZM output can be written as

$$E_{MZM}(t) = \sqrt{P(t)}e^{j2\pi f_o t} \cdot \cos\left(\frac{\pi}{2}\frac{V_{BIAS}}{V_\pi}\right) - \sqrt{P(t)}e^{j2\pi f_o t}\frac{\pi}{2V_\pi} \cdot \sin\left(\frac{\pi}{2}\frac{V_{BIAS}}{V_\pi}\right)s(t)$$

which, for $V_{BIAS} = V_\pi/2$ becomes

$$E_{MZM}(t) = \frac{\sqrt{2}}{2}\sqrt{P(t)}e^{j2\pi f_o t} + \frac{\sqrt{2}\pi}{4V_\pi}s(t)\sqrt{P(t)}e^{j2\pi f_o t} = \frac{\sqrt{2}}{2}x(t) + \frac{\sqrt{2}\pi}{4V_\pi}s(t)x(t).$$

Finally, the output current $i_{PIN}(t)$ of the photodiode is

$$i_{PIN}(t) = R \cdot |E_{MZM}(t)|^2$$

which, after some math becomes

$$i_{PIN}(t) = \frac{R}{2}P(t) + \frac{R}{2}P(t) \cdot \frac{\pi}{V_\pi}s(t)$$

where

- R represents the responsivity of the photodiode.

The system depicted in Fig. 3 has been simulated with OptiSystem and the obtained spectra are shown in Fig. 4. The OFDM central frequency is 10 GHz, and a Gaussian distributed optical white noise at 1550 nm wavelength has been filtered around the central wavelength with a bandwidth of 2 GHz to be used as SUT. Even though the SUT spectrum has been fully recovered after the photodiode, it can be seen that the resolution level has not been improved as expected. In fact, the signal spectrum obtained after photodetection corresponds to the cross-correlation of the OFDM and SUT spectra. Therefore, modulating the SUT with the OFDM signal does not guarantee the recovery of its spectrum in a controlled manner and a different approach must be considered.

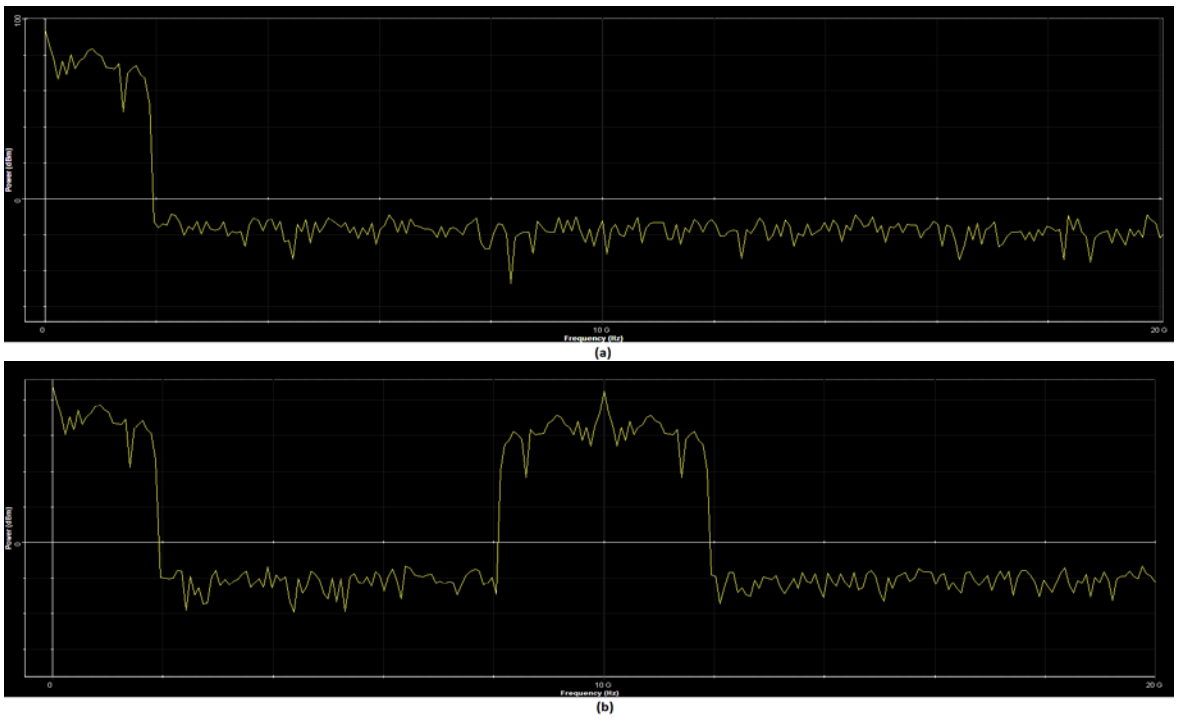

Fig. 4. 2-GHz optical spectrum detected by a PD, before (top) and after (bottom) being modulated with the OFDM signal.

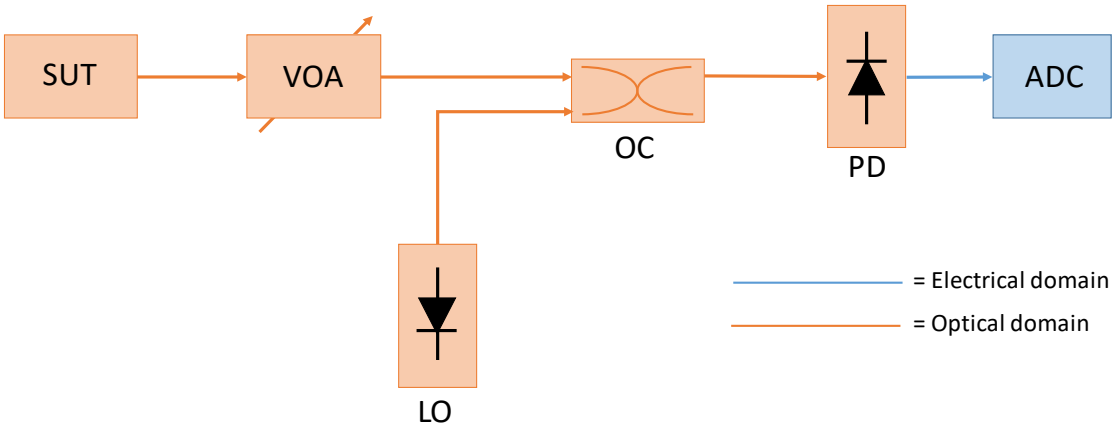

Fig. 5. Simplified block diagram of the coherent approach. SUT: signal-under-test, VOA: variable optical amplifier, LO: local oscillator, OC: optical coupler, PD: photodetector, ADC: analog-to-digital converter.

A new scheme is currently under investigation and involves the use of a coherent receiver, as depicted in Fig. 5. The idea behind it is to exploit the local oscillator (LO) sweeping its frequency across the measurement wavelength range. After having coupled the LO with the SUT by means of an optical coupler (OC), the resulting signal is detected by an avalanche photodiode (APD) with a limited bandwidth (100 MHz - 1 GHz) according to the desired spectrum resolution.

Future steps regarding this approach will include its validation by means of simulation software (i.e. VPI): if the expected improved resolution of the SUT spectrum will be confirmed by the simulation's results, then a further experimental validation could be carried out in the lab.

4 OPTICAL SPECTRUM PROCESSING AND ANALYSIS

As mentioned in Section 2, one of the most common method to measure the OSNR of an optical signal, employs OSA. By interpolating the noise level at the two adjacent sides of the considered channel, OSA allows the measurement of the ASE noise introduced by the optical amplifiers in the channel itself. Issues arise when wavelength switched optical networking or the ultra-dense wavelength division multiplexing (ultra-DWDM) scenarios are considered. In the first case, each channel could exhibit a different noise level, as it may have experienced a different route compared to the others. On the other hand, in the second case, the noise level between two adjacent spectral channels could not represent their real noise level, but instead their overlap. Furthermore, along their path towards the receiver, each signal could cross a certain number of reconfigurable optical add/drop multiplexers (ROADMs), namely several optical filters. Direct effect of the filters presence is the sharp drop of the noise floor between the channels, making its measurement challenging. Another consequence, especially in long-haul topologies, where the filter cascade effect (FCE) assumes a crucial role, is the further tightening of the filters pass-band through which the original signal shall pass, resulting in a signal distortion.

Thus we tried to identify a method that, despite the above mentioned challenges, could return a reliable estimation of the signals OSNR starting from their optical spectra. In addition, we also tried to understand whether the optical spectra resolutions had an impact on the estimation accuracy. To do so, we took advantage of the high-resolution spectral images that BOSA can guarantee (see Section 3). Indeed, BOSA provides optical spectral resolutions up to 0.1pm (about 10MHz), certainly finer than those offered by the classic diffraction grating based OSAs, which range in the order of 0.01nm (about 1GHz). Relying on optical spectra with such high degree of definition, theoretically should allow us to identify the noise level of a specific channel more precisely with respect to a standard OSA approach, therefore enabling a more accurate OSNR estimation.

Fig. 6 depicts the experimental setup, performed in the CTTC optical lab, through which several high-resolution optical spectra were captured. It shows a 28GBd PM-QPSK modulated signal, generated from a tunable laser working at 1550.918nm (193.3008THz) and transmitted over 5 different paths: back to back (B2B), 35km, 50km, 150km and 250km. Each one of these five scenarios has been implemented exploiting the ADRENALINE testbed available at the CTTC premises. At the output of the testbed, a variable optical attenuator (VOA) has been placed before an amplification stage, emulating 16 different OSNR values (e.g. from 0 to 30dB). Finally, the spectra of the transmitted signals have been acquired using the BOSA.

Fig. 6. Schematic diagram of the experimental setup for the high-resolution optical spectra acquisition. PM-IQ-MOD: polarization multiplexed-IQ-modulator, DAC: digital-to-analog converter, VOA: variable optical attenuator, BOSA: Brillouin optical spectrum analyser.

For each scenario, a total of 160 optical spectra have been collected, specifically 10 for each VOA level (5 for each polarization state).

Once captured, the high-resolution optical spectra have been imported and post-processed in MATLAB and their corresponding low-resolution versions have been obtained. An example of an optical spectrum acquired by the BOSA with its relative post-processed low-resolution case is shown in Fig. 7. All the details relative to the developed MATLAB tool are presented (and discussed) at the end of this document in Appendix A. Basically, what the algorithm returns is a set of features that define each optical spectrum: central frequency, 3dB-bandwidth and OSNR value.

Having available the whole set of captured spectra with two different resolutions, allowed us to compare the results returned by the developed tool for the two analysed resolution scenarios. Theoretically, it is expected a greater effectiveness of the algorithm if high-resolution optical spectra are chosen. However, the actual results of our simulations show that there are no substantial differences between high and low-resolution cases, at least for the features that we have considered.

Every time the optical signal enters or leaves one of the ADRENALINE testbed nodes, it also passes through an optical filter. In our case, the 35km and 50km configurations include optical filters with 100GHz-bandwidth, while for the 150km and 200km scenarios the bandwidth of the filters range between 50GHz and 100GHz. Thus, during the post-processing phase, the spectra relative to the signals of B2B, 35 km and 50km cases have been furthered filtered using a 50GHz-bandwidth optical filter, to check whether some differences between the two resolutions arise. The adopted filter, which has been characterized at CTTC lab, is shown in Fig. 8. In Fig. 9 the filtered signal is depicted together with its original pre-filtered version at the two considered resolution values: 0.1pm (a) and 0.01nm (b). As expected, the filter presence affected the real noise level outside the signal bandwidth, thus the algorithm has not been able to identify the correct OSNR values. Again, no substantial differences were found between the two analysed resolutions. Therefore, a further step has been performed, considering a machine learning (ML)-based approach.

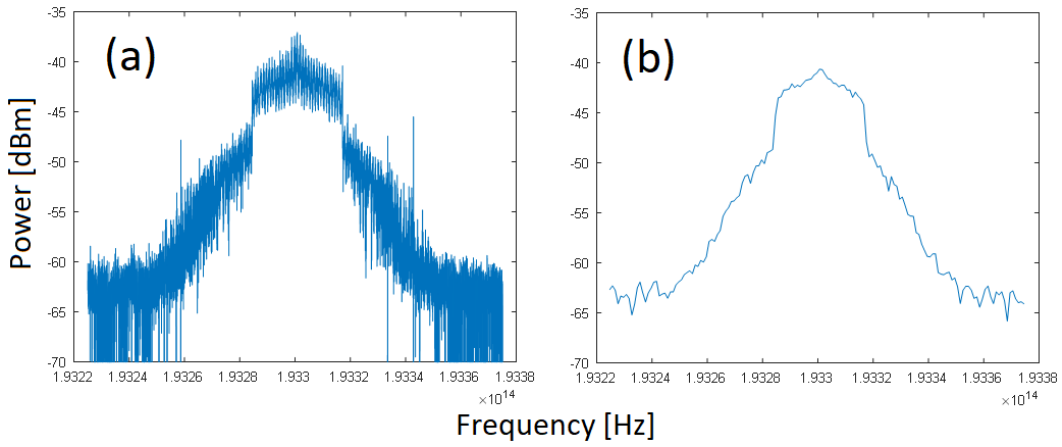

Fig. 7. Example of optical spectrum acquired by the BOSA at 0.1pm (a) and its corresponding low-resolution version at 0.01nm obtained by post-processing the original spectrum in MATLAB (b).

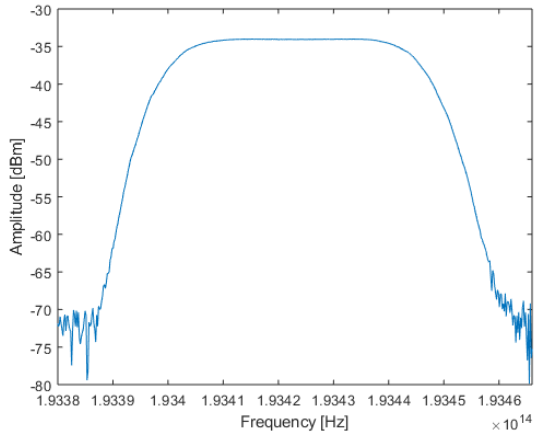

Fig. 8. Frequency response of the applied 50GHz-bandwidth filter centred at 1550nm.

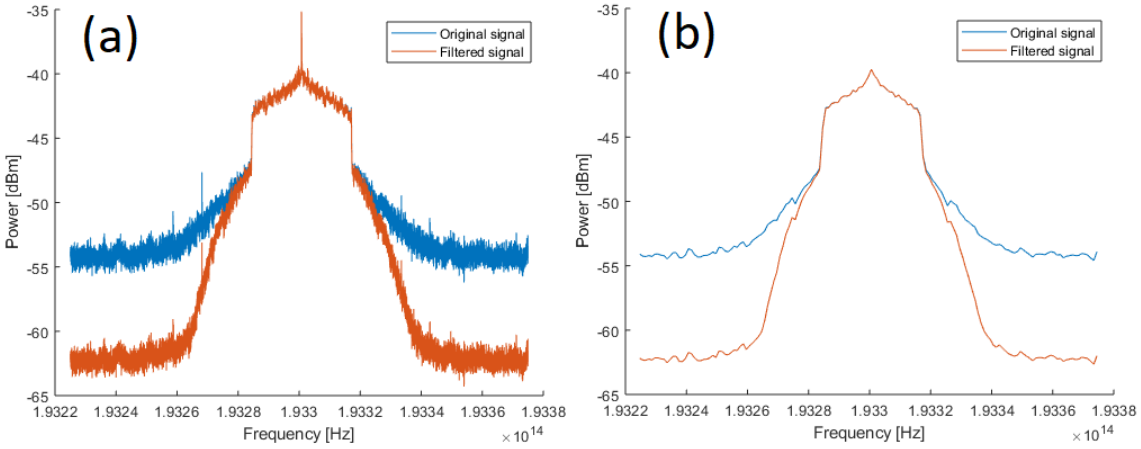

Fig. 9. Original (blue) and filtered (orange) optical spectrum at high (a) and at low-resolution (b).

4.1 OSNR IDENTIFICATION WITH MACHINE LEARNING

Machine learning (ML) is assuming a relevant role in lot of scientific fields and is also becoming more and more attractive in the optical communication context. In [24], the authors considered 4 common ML algorithms (support vector machine (SVM), artificial neural network (ANN), k-nearest neighbours (KNN) and decision tree) and among them they identified SVM as the most promising approach for OSNR analysis. Based on this premise, we consider this approach and feed the SVM algorithm with our set of spectral data. Before doing this, the spectra have been processed to produce a variety of scenarios, such as: different filter extinction ratio, laser drift, filter tilt and filter tightening. Each spectrum of the training data set is associated with its relative OSNR reference value, previously calculated (see Appendix A for more information about how the reference OSNR values were obtained). Spectra representing signals with OSNR reference values lower than 8dB have been excluded a priori from both the training and the testing data set, since in real optical system such low OSNR signals would not be considered as valid.

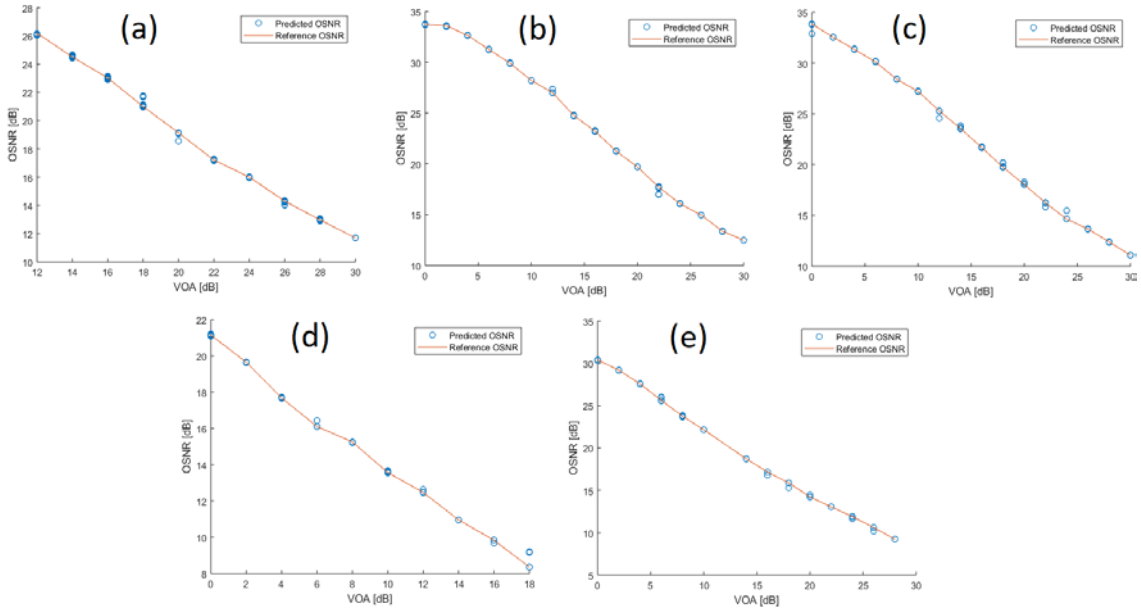

Fig. 10. Reference and predicted OSNR values as function of the VOA levels in the high-resolution case for different distances scenario: (a) B2B, (b) 35km, (c) 50km, (d)150km and (e) 200km.

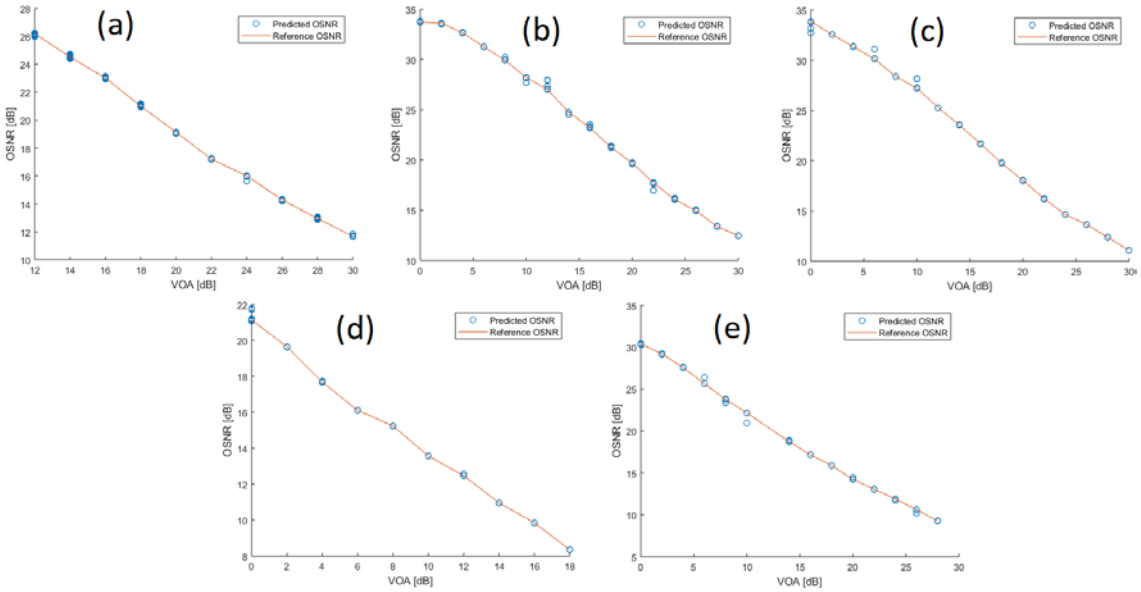

Fig. 11. Reference and predicted OSNR values as function of the VOA levels in the low-resolution case for different distances scenario: (a) B2B, (b) 35km, (c) 50km, (d)150km and (e) 200km.

In addition, since data processing speed is a fundamental aspect of ML algorithms [24], the spectra have been cut at the edges of the PM-QPSK modulated signal, to ensure that their dimension did not affect the computation time. Furthermore, this cutting operation allowed us to replicate a real WDM spectrum where each channel is bounded by the adjacent ones, thus resulting in a very narrow area for OSA to detect the desired signal spectrum. In the high-resolution case, each spectral data provided to the SVM algorithm

was represented as a column vector of size (1, 24000), whereas in the low-resolution case the vector size was (1, 48). The total amount of spectra fed to the algorithm was 198: of these, 169 were used to train it, whereas the remaining 29 for testing it, with a ratio between training and test data of almost 6:1. The obtained results are reported in Fig. 10 and in Fig. 11: the reference OSNR values and those predicted by the SVM algorithm are shown as function of the different VOA levels for the high and low-resolution case respectively. Furthermore Fig. 12, shows the probability density functions (PDFs) of the error (in dB) made by the SVM algorithm while predicting the OSNR values with respect to those calculated as reference. In the figure insets, the mean squared error (MSE) and the maximum error (MAX) values of each scenario are also highlighted.

For a final validation of the achieved results, several VPI-based simulations were carried out with the purpose of collecting additional sets of optical spectra. The main reason of this further check was done to verify if all the processing applied a posteriori to the original collected BOSA spectra has influenced in some ways the obtained results.

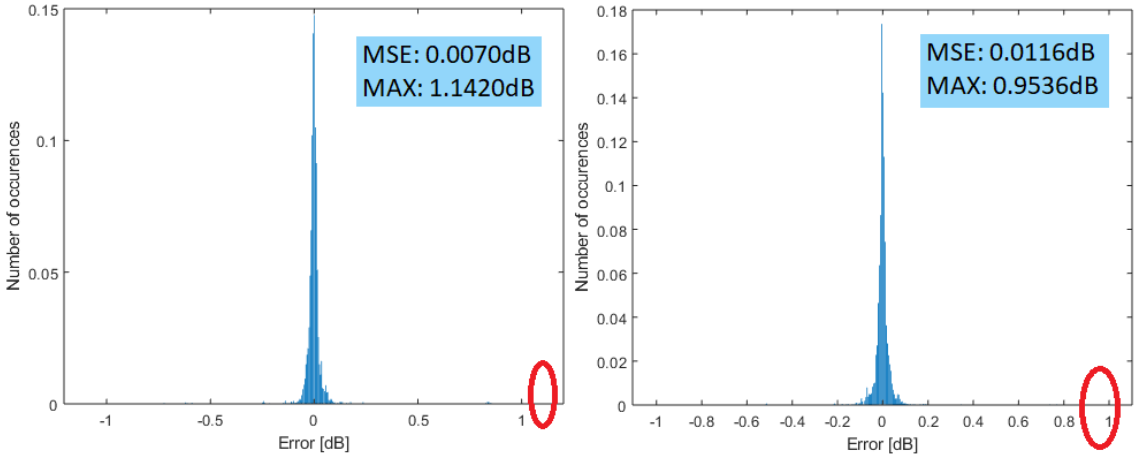

Fig. 12 Probability density functions of the error committed by the SVM algorithm while predicting the OSNR for (a) the high-resolution and (b) the low-resolution cases. For both the cases the maximum error is highlighted in the red circle.

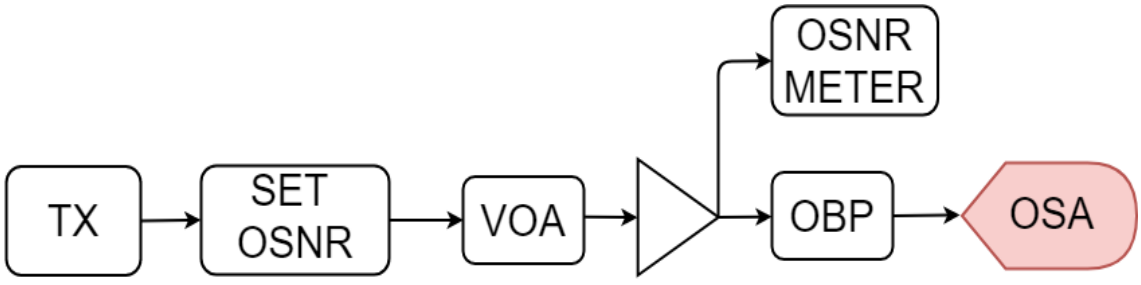

Fig. 13. Schematic diagram of the VPI simulation setup. TX: optical transmitted signal, VOA: variable optical attenuator, EDFA: erbium-doped fiber amplifier, OBP: optical bandpass filter, OSA: optical spectrum analyser.

Unlike the experimental case, this time the only considered scenario was B2B. Fig. 13 shows the VPI simulation setup in which two different modulation formats have been used: polarization multiplexed QPSK (PM-QPSK) and polarization multiplexed 16QAM (PM-16QAM). In the former case, a 112Gb/s PM-QPSK signal is generated and its OSNR is adjusted with an OSNR set module, which adds further noise to the input signal till the targeted OSNR level is reached. After passing through a variable optical attenuator (VOA) and an erbium-doped fiber amplifier (EDFA), the OSNR values that will be used as reference are measured by an OSNR meter. A second order Gaussian optical filter emulates the filtering effect that the signal experiences when passing through the different ROADM nodes. Two different filter bandwidths have been considered: 37.5GHz and 50GHz. Finally, the spectral data are collected by an OSA module configured with 10MHz and 1GHz resolutions. The VOA has been swept with 2dB steps, in a range between 0 and 30dB, exactly as it was in the experimental case. In addition, the filter bandwidth has been modified in order to emulate two specific soft failure scenarios: the filter shift and the FCE. The former case, applied to both the filter bandwidth values (37.5GHz and 50GHz), has been reproduced by shifting the filter central frequency of ± 1GHz with respect to the signal central frequency. On the other hand, FCE was considered only for the 37.5GHz bandwidth case and has been emulated reducing the bandwidth of the optical filter to 35GHz, 30GHz and 25GHz. Furthermore, to reproduce the laser drift failure scenario the spectral data have been cut at the signal edges at a random frequency value in the range of ± 1GHz. For each of the two resolution levels (10MHz and 1GHz), a total of 144 optical spectra has been generated and collected through VPI (96 with the filter configured with 37.5GHz bandwidth and 48 with the filter at 50GHz). Exploiting the same VPI setup of the previous case, a 224Gb/s PM-16QAM signal have also been generated. However, unlike the previous situation, this time only the 37.5GHz bandwidth filter configuration was considered. In addition, the filter's shifting values covered both the ± 1GHz and ± 2GHz cases. All the other settings have been maintained as for the previous modulation format experiment. Under these circumstances, a total of 128 optical spectra have been collected for each one of the two resolution scenarios. In both cases, the 85% of the collected spectral data were used to train the SVM algorithm, while the remaining 15% was used to test it. Each spectrum of the training data set is associated with its relative OSNR reference value measured by the OSNR meter while collecting the spectra. Fig. 14 and Fig. 15 report the obtained results for the PM-QPSK and PM-16QAM modulation formats respectively. The pictures illustrate the PDF of the error (in dB) made by the SVM algorithm while predicting the OSNR values with respect to those measured by the OSNR meter and used as reference. In the figure insets, the mean squared error (MSE) and the maximum error (MAX) values of each scenario are also reported. The results are promising and show that the maximum OSNR error estimation is maintained lower than 0.4dB in every considered scenario (different resolution, filter bandwidth and modulation format).

The work related to the ML-based OSNR estimation approach described in 4.1 section, has been also reported in [2], a letter submitted to IEEE Photonic Technology Letters (PTL) and currently under revision.

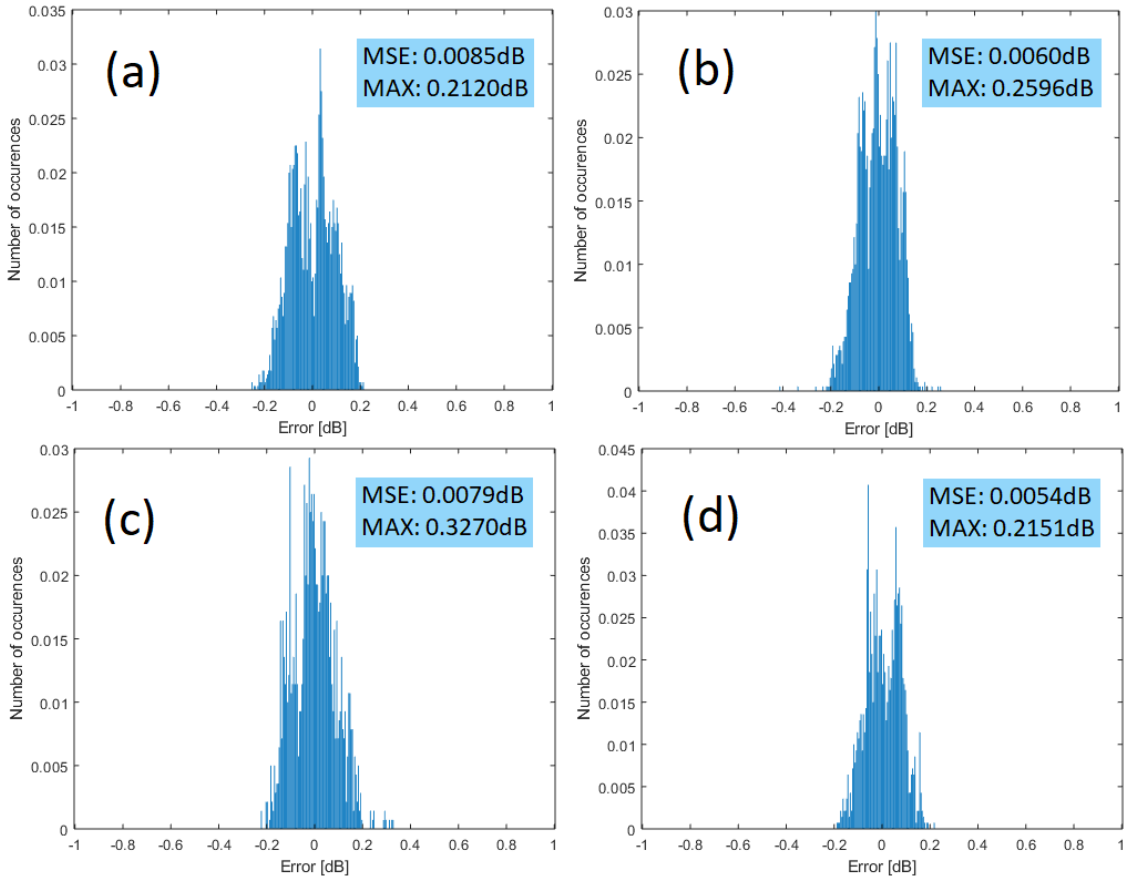

Fig. 14. Probability density functions of the error committed by the SVM algorithm while predicting the OSNR using PM-QPSK as modulation format. The pictures report the error's PDF, MAX and MSE in case of spectral data obtained at: (a) high-resolution (10MHz) and an optical filter bandwidth of 37.5GHz, (b) low-resolution (1GHz) and an optical filter bandwidth of 37.5GHz, (c) high-resolution (1GHz) and an optical filter bandwidth of 50GHz, (b) low-resolution (1GHz) and an optical filter bandwidth of 50GHz.

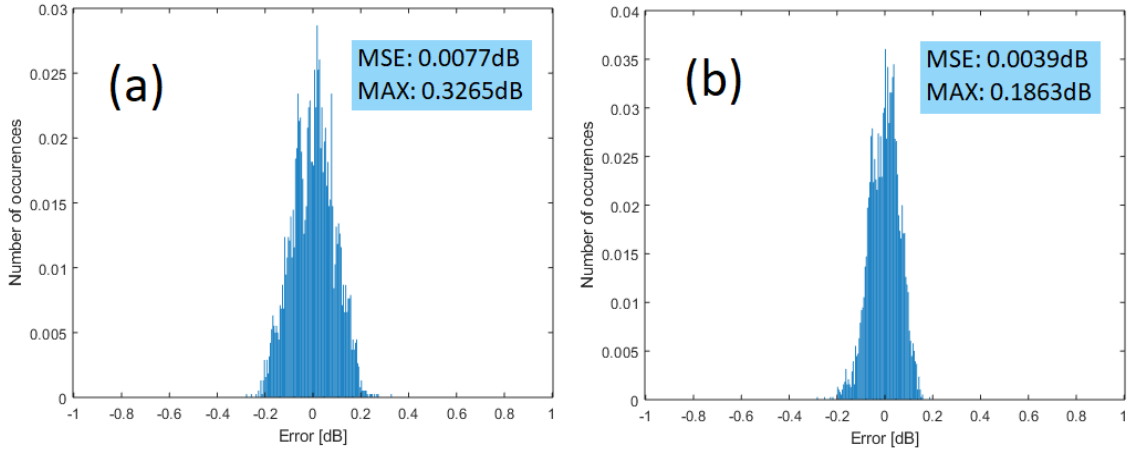

Fig. 15. Probability density functions of the error committed by the SVM algorithm while predicting the OSNR using PM-16QAM as modulation format for (a) the high-resolution and (b) the low-resolution cases.

5 CONCLUSIONS AND FUTURE PLANS

Since he joined ONFIRE project on May 2018, ESR1 has been involved in WP1 activities, including the SoA analysis to enable identifying open problems and methods leading to the ONFIRE goals. The results of these activities led to the production of a consolidated SoA survey and individual research proposal of ESR1 (included in D1.1 [1]). In particular, a deep study of three main subjects was conducted: low-margin optical networks, OSNR monitoring techniques and disaggregated optical networks. Within the report drafting, for each of the above-mentioned topics, a large amount of literature was reviewed. The SoA elaboration has allowed the ESR to develop a procedure for searching, reading and understanding the works done so far in the literature, making him able to identify potential gaps and thus pursuing new possible lines of research and defining an individual research proposal. In particular, for what concern the study and development of cost-effective solutions for non-intrusive in-band performance monitoring, the ESR1 during this first year has been involved in the design of a low-cost scheme for high-resolution signal spectrum analysis, as reported in Section 3. Moreover, with regards to the processing and analysis of the spectral data, ESR1 has developed an algorithm able to understand, under certain circumstances, several spectral features that define the optical spectra, such as their OSNR, their central frequency and their bandwidth. This method returned satisfactory results which worsened once the filtering effects were considered. Thus, in addition to this approach a machine learning-based method for OSNR estimation was developed relying on the SVM algorithm. The two solutions, reported in Section 4, exploited the high-resolution spectral data previously captured in CTTC lab by means of the BOSA, which were processed to obtain their low-resolution version. Both the two resolution variants were then fed to the machine learning algorithm. The results were promising and showed that the OSNR was estimated by the SVM algorithm with quite good precision in both the resolution scenarios, exhibiting slightly better error margins in the high-resolution case. For a further validation of this approach, additional spectral data at different modulation formats and with different optical filter bandwidth values were generated by means of VPI and fed to the SVM algorithm. The results proved that the algorithm can identify the OSNRs with even a lower error margin than in previous cases, since the VPI produced/simulated spectral data are definitely better shaped and have a less-realistic form.

So far, the achieved goals match those planned, but certainly many further steps are planned for the future. Short-term objectives include the collection of further experimental spectral data with different optical filter bandwidth values and possibly with a different modulation format for further testing the ML-based OSNR estimation tool. Another task to be accomplished in the near future is the validation of the approach proposed in section 3 by means of software simulations and, if these return promising results, also in the lab. Regarding the activities to be developed in the long-term, an important role could be played by the integration of the developed ML-based OSNR monitoring approach with the margin reduction scenario. This task could also envisage a possible collaboration with ESR2. Furthermore, the developed OSNR monitoring technique could also be leveraged to reduce the possible side-effects introduced by the disaggregation in the optical network. Finally, since the knowledge of the signal 3dB-bandwidth can help

to understand the effects of the filters over the signal itself, the monitoring of this parameter could allow a better network automation. Thus, another possible long-term goal include the development of a ML-based approach to estimate the signals 3dB-bandwidth starting from their optical spectra.

6 REVIEW AND FEEDBACK FROM ADVISORY COMMITTEE

The comments received by the Advisory Committee (AC) regarding the deliverable D1.1 submitted on December 2018 are reported below.

Name of the Reviewer: *Dr. Paola Parolari*

General comments on the deliverable:

The SoA analysis is clear and comprehensive for the topics taken into account.

-In Section 6 the objective and expected results are described, however I suggest to outline them more clearly and to provide the methodology and timeline of the activities in order to obtain a clear research plan.

Answer: a new section called "Planning and Methodologies" was added at the end of the deliverable to provide an overview on the methodology of work and on the envisioned time work plan. Also, a draft Gantt chart was attached to the deliverable. These additions were done before submitting the deliverable.

Minor comments on formal aspects:

I suggest to check throughout the document the section numbers (e.g. pag 8), blank paragraph after bullets (e.g. pag 23-25), and Figures in-between sentences (e.g. pag 29, 35, 39).

Answer: We proof-read the deliverable before submitting it. Most of the typos, including the one mentioned by the reviewer were corrected.

Name of the Reviewer: *Dr. Prof. Andreas Kirstädter*

General comments on the deliverable:

- Details of the research proposal are missing as well as timeline and milestones

Answer: as outlined above, we added a new section called "Planning and Methodologies" at the end of the deliverable before submitting it. Also, the research proposal terms were specified in more detail in section 3, "Objectives to be achieved".

- State-of-the-art of SDN and NFV for EON is missing

Answer: We argue that these topics are out of the scope of ESR1 Ph.D. This decision and all the other changes to D1.1 were also presented during the general meeting that took place at CTTC in January 2019, in the presence of ESR1 supervisors and were discussed also with the AC members and P.

- Example values for typical margins in systems would support understanding the problem

Answer: example values for typical margins were added in the low-margin optical network section.

- Typical durations of soft failures in current systems and intended values for the future would support understanding the problem

Answer: Soft failure are a research topic and as so there are no specific values that we can reference for real systems. Researchers are currently studying various flavours of soft failures, which might come from long term effects, i.e. optical equipment ageing, which is a slow process that can be foreseen and the restoration could be precalculated, or some faster term impairment effect where the calculations have to be reactive. The calculation is typically not the slowest part, the control plane of existing optical networks requires minutes to establish or reconfigure connections. Dynamic restoration also takes minutes. So, we could set a similar target for soft-failures.

-It should be explained why the research of novel flexibel transmission technologies is required and how this does relate to the project objectives --> wouldn't be the effort for this research too much?

Answer: The reviewer is correct in that research in transmission technologies might make the topics that are studied by the ESR1 too wide. This direction was included in the initial plan of ESR1, and for the time being it is left for future, and it might not be followed depending on the difficulties and time of the other topics studied by ESR1.

7 APPENDIX A - DEVELOPED "TOOL"

The collected set of spectra originally consisted of 160 spectra for each distance scenario: 10 for each of the 16 VOA levels. In particular, each of these 16 subsets of 10 spectra was composed by 2 group of 5 spectra each, which represent the two polarization state of the signal. These 5 spectra simply represented 5 different captures obtained with the same configuration. For every path scenario, our goal was to finally have one single spectrum for each VOA level. To do so, we first averaged the 5 equal captures to get a time average of each spectrum and then we simply added the two different spectra representing the two polarization state. All the operations were done in the linear domain.

As mentioned in Section 4, the original resolution of the collected BOSA spectra was around 10 MHz, therefore to worsen this value and thus obtain the low resolution version of the spectral data, we processed them in MATLAB. To do so, several functions were considered, among which: "movmean", "mean", "downsample" and "max". While in "movmean" the window on which the mean is calculated slides across the original vector, in "mean" this window is hardly shifted of a fixed amount of points. Thus, "movmean" guarantees a higher number of points whereas "mean" follows the original spectrum evolution with a better accuracy. On the other hand, the function "downsample" just takes one value every block of x points whereas "max" selects the maximum value inside the same block. After some trials we identified "mean" as the better option to reduce the spectral resolution as realistically as possible. Hence, through this procedure the spectra size has been reduced from 187288 samples, relative to the high-resolution scenario, to 375 samples, for each spectrum.

Once we got the spectra at both the desired resolution values, we started developing the actual algorithm with the following purposes: central frequency and 3-dB bandwidth identification and OSNR estimation. To accomplish the first task (i.e. central frequency identification) we considered the high-resolution spectra: since all the considered spectra exhibited the carrier, through a peak detection function we managed to spot their associated frequencies, which then have been collected as the signals central frequencies. Once the center of the channel slot was detected, a smoothed version of the spectrum was considered. To do so, a low-pass filter was applied to the original spectral data filtering out its high-frequency components. Therefore, frequency pairs corresponding to the edges of various x-dB bandwidth were identified. This process, started at the level of the detected central frequency and allowed us to descend along the signal curve, ending once the noise level was approached. Such procedure also enabled the OSNR estimation, since the difference between the initial amount of power and the one reached at the end of the process represented an approximation of the OSNR.

On the other hand, the reference OSNR was calculated by means of the integral method on the high-resolution linear spectral version of the signals. Two integration bandwidth spans were defined: one relative to the signal calculation, which was set to 0.4nm (50GHz) and one for the noise calculation, set at 0.1nm (12.5GHz). The integration over the first bandwidth was centered around the previously identified central frequency and returned the sum between the signal and the noise powers. Thus, a second integration was performed, this time centered in the noise region, to calculate only the noise power level

within the same signal bandwidth. This value was then subtracted from the first integration result, leading to the exact signal power amount. Finally, a last integration centered in the noise region was performed within the noise bandwidth, resulting in the noise power level. The two obtained power amounts, the signal and the noise one, were then divided giving the reference OSNR value.

Regarding the introduction of the filter in the system, we first imported the filter file and then multiplied its values for the ones of the initial spectra. Once each single spectrum was filtered, we performed the average over the time (averaging the 5 repeated samples) and finally the linear sum of the two polarization state, as described in the paragraph above.

8 REFERENCES

[1] F. Locatelli, J. M. Fàbrega, M. Svaluto Moreolo, K. Christodoulopoulos, F. Buchali, and S. Spadaro, "D1.1: Consolidated state of the art survey and individual research proposal," 2018.

[2] F. Locatelli, K. Christodoulopoulos, M. Svaluto Moreolo, J. M. Fàbrega, and S. Spadaro, "Machine Learning Approach for in-band OSNR Estimation from Optical Spectra," submitted to *Photonics Technology Letters*, 2019.

[3] R. Muñoz *et al.*, "D4.5: Progress report," 2018.

[4] B. Chomycz, Planning Fibre Optic Networks. 2009.

[5] J. H. Lee, H. Y. Choi, S. K. Shin, and Y. C. Chung, "A review of the polarization-nulling technique for monitoring optical-signal-to-noise ratio in dynamic WDM networks," *J. Light. Technol.*, vol. 24, no. 11, pp. 4162–4171, 2006.

[6] Zhenning Tao, Zhangyuan Chen, Libin Fu, Deming Wu, and Anshi Xu, "A novel method to monitor OSNR using a Mach-Zehnder interferometer," Tech. Dig. CLEO/Pacific Rim 2001. 4th Pacific Rim Conf. Lasers Electro-Optics (Cat. No.01TH8557), vol. 2, p. II-564-II-565.

[7] S. K. Shin, K. J. Park, and Y. C. Chung, "A novel optical signal-to-noise ratio monitoring technique for WDM networks," *Opt. Fiber Commun. Conf. Tech. Dig. Post-conf. Ed. Trends Opt. Photonics Vol.37* (IEEE Cat. No. 00CH37079), vol. 2, pp. 182–184.

[8] J. H. Lee, N. Yoshikane, T. Tsuritani, and T. Otani, "In-band OSNR monitoring technique based on link-by-link estimation for dynamic transparent optical networks," *J. Light. Technol.*, vol. 26, no. 10, pp. 1217–1225, 2008.

[9] N. Hanik, A. Gladisch, C. Caspar, and B. Strebel, "Application of Amplitude Histograms to Monitor Performance of Optical Channels," *Electron. Lett.*, vol. 35, no. 5, pp. 403–404, 1999.

[10] R. S. Luis, L. Costa, A. Teixeira, and P. André, "Optical performance monitoring based on asynchronous amplitude histograms," in *Optical Performance Monitoring*, C. C. K. Chan, Ed. Elsevier, 2010, pp. 145–174.

[11] J. H. Lee and Y. C. Chung, "Optical signal-to-noise ratio monitoring," in *Optical performance monitoring*, C. C. K. Chan, Ed. Elsevier, 2010, pp. 21–66.

[12] Z. Dong, F. N. Khan, Q. Sui, K. Zhong, C. Lu, and A. P. T. Lau, "Optical Performance Monitoring: A Review of Current and Future Technologies," *J. Light. Technol.*, vol. 34, no. 2, pp. 525–543, 2016.

[13] Z. Dong *et al.*, "Optical performance monitoring in DSP-based Coherent Optical Systems," in *Optical Fiber Communication Conference* 2015.

[14] Y. Pointurier, "Design of Low-margin Optical Networks," *Opt. Fiber Commun. Conf.*, vol. 9, no. 1, p. Tu3F.5, 2016.

[15] J.-L. Auge, "Can we use Flexible Transponders to Reduce Margins?," *Opt. Fiber Commun. Conf. Fiber Opt. Eng. Conf. 2013*, p. OTu2A.1, 2013.

[16] S. Perrin, "Bringing Disaggregation to Transport Networks," *Heavy reading, Fujitsu*, 2015.

[17] J. Donovan, “Hitting the Open Road: Software-Accelerating Our Network with Open Source,” *AT&T Innovation Blog*, 2015. [Online]. Available: https://about.att.com/innovationblog/061714hittingtheopen.

[18] J. M. Fàbrega, M. Svaluto Moreolo, and L. Nadal, “Optical Performance Monitoring Systems in Disaggregated Optical Networks,” 2018, pp. 1–4.

[19] M. De Leenheer, T. Tofigh, and G. Parulkar, “Open and Programmable Metro Networks,” *Opt. Fiber Commun. Conf. 2016*, pp. 3–5.

[20] E. Riccardi, P. Gunning, O. S. G. L. De Dios, M. Quagliotti, V. Lopez, and A. Lord, “An Operator view on the Introduction of White Boxes into Optical Networks,” *J. Light. Technol.*, vol. 36, no. 15, pp. 3062–3072, 2018.

[21] J. M. S. Domingo, J. Pelayo, F. Villuendas, C. D. Heras, and E. Pelllejer, “Very high resolution optical spectrometry by stimulated Brillouin scattering,” *IEEE Photonics Technol. Lett.*, vol. 17, no. 4, pp. 855-857, 2005.

[22] A. Photonics, “BOSA Technology.” [Online]. Available: https://aragonphotonics.com/bosa-technology/.

[23] J. Leibrich, A. Ali, H. Paul, W. Rosenkranz, and K. D. Kammeyer, “Impact of modulator bias on the OSNR requirement of direct-detection optical OFDM,” *IEEE Photonics Technol. Lett.*, vol. 21, no. 15, pp. 1033-1035, 2009.

[24] D. Wang, *et al.*, “Machine Learning-Based Multifunctional Optical Spectrum Analysis Technique,” *IEEE Access*, vol. 7, pp. 19726-19737, 2019.